Reverse micelle strategy for effective substitutional Fe-doping in small-sized CeO2 nanocrystals: Assessment of adsorption and photodegradation efficiency of ibuprofen under

MethodsX 8 (2021) 101463

Contents lists available at ScienceDirect

MethodsX

journal homepage: www.elsevier.com/locate/mex

Method Article

Method for fluvial and pluvial flood risk assessment in rural settlements

Maurizio Tiepolo[a,*], Elena Belcore[b], Sarah Braccio[a], Souradji Issa[c], Giovanni Massazza[d], Maurizio Rosso[b], Vieri Tarchiani[e]

[a] *DIST-Politecnico and University of Turin, Italy*
[b] *DIATI-Politecnico of Turin, Italy*
[c] *Ministry of Agriculture and Livestock, Niger*
[d] *AIPO-Interregional Agency for Po River, Moncalieri, Italy*
[e] *Institute of Bio Economy, National Research Council, Italy*

A B S T R A C T

Flood risk assessments in the Global South have increased since the adoption of the United Nations Sendai Framework for Disaster Risk Reduction 2015–2030. However, they often fail to meet disaster risk reduction needs at the local scale, because they typically consider only one hazard (fluvial or pluvial floods). Furthermore, hazard and exposure are considered as stationary conditions, flood-prone assets are rarely identified, risk reduction measures are not identified in detail for specific locations, and the convenience of reducing or accepting risk is not evaluated. This paper describes a flood risk assessment method that is innovative in that it considers three hazard types (backwater, fluvial, and pluvial floods) and multiple risk scenarios; it uses orthophotos generated from images captured by an unmanned aerial vehicle and very high-resolution satellite images, and it involves communities in risk assessment. The method was applied to four rural settlements along the Sirba River, Niger. The assessment identifies the benefit of reducing risk in monetary terms, as well as the intangible benefits that reducing risk could generate, and it detects opportunities that flooding offers for rural development. The method can be replicated in all contexts where decision-making support is needed for flood risk assessment planning.

- Risk analysis and evaluation is participatory.
- Risk assessment is improved by combining local and technical knowledge.
- Assets are identified using very-high-resolution satellite and drone images.

* Corresponding author.
E-mail address: maurizio.tiepolo@polito.it (M. Tiepolo).

https://doi.org/10.1016/j.mex.2021.101463

ARTICLE INFO
Method name: Risk management, risk assessment techniques
Keywords: Damage, Disaster risk reduction, Hydraulic modelling, Local knowledge, Multi-hazard, Public participation, Unmanned aerial vehicle, VHR satellite images
Article history: Received 11 May 2021; Accepted 19 July 2021

Specifications table

Subject Area	Engineering
More specific subject area	Disaster risk reduction
Method name	Risk management, risk assessment techniques
Name and reference of original method	ISO 31010 Risk management–risk techniques Occasional flood risk assessments
Resource availability	River discharge and flood prone assets: doi: 10.17632/c8h23xms5w.1 Images: Google Earth and Unmanned Aerial Vehicle

Over the last 30 years, floods have become more frequent, even in semi-arid rural areas [1]. The United Nations Sendai Framework for Disaster Risk Reduction (SF) was developed to significantly increase knowledge of risk and local risk reduction strategies in member countries by 2030 [2]. One of the effects of this commitment has been an increase in peer-reviewed literature on flood risk in rural regions of the Global South. However, this literature remains of little use in reducing risk locally. Flood risk assessments (FRAs) tend to consider a single hazard at a time. Hazards and exposed assets are rarely detailed [3]. Most FRAs do not consider erosion processes, cultural changes, and incessant anthropogenic pressure in rural areas [26] that alter catchments within a few years and consequently modify discharge [5]. Furthermore, the spectrum of risk treatment benefits is still limited and rarely considers intangible benefits and opportunities offered by floods in semi-arid contexts [6]. Many of these shortcomings are due to the poor accuracy of information provided by global datasets on pluviometry, land use/land cover, and flood damage at the local scale. This limitation can be circumvented, integrating local knowledge [7] with scientific and technical knowledge.

The proposed method, which is based on the participation of local communities and authorities, integrates local knowledge, hydraulics, geomatics, and risk management techniques. Furthermore, risk reduction policies are determined in accordance with ISO 31010 [8]. The innovations proposed in conjunction with this improved FRA method include the systematic integration of local and technical-scientific knowledge, the use of images captured by unmanned aerial vehicles (UAV), very high-resolution (VHR) satellite imagery, and the production of risk scenarios [9] that include the opportunities offered by floods. Fluvial and pluvial FRAs were conducted in four phases: context definition, risk identification, analysis, and evaluation (Fig. 1).

The first phase establishes the requirements for a multi-hazard risk analysis, criteria for calculating the probability of flooding, flood scenarios, and information required to decide whether to treat or accept the risk. Multi-hazard analysis requires the same dataset length, the same asset identification procedure and precision, and the same approach to computing asset value [10]. The risk (R) is the product of the hazard (H) and potential damage (PD), i.e., $R = H \times PD$. Flood scenarios are then determined based on the probability of occurrence (frequent, moderate, or rare) and the condition of the catchment (provided with or without risk reduction measures).

In the second phase, the hydro-climatic threats, past catastrophic events, and critical flood level over which damages are produced are identified through meetings with flood-prone communities. Historical data on river discharge, rainfall, and the extension of the settlements are considered in assessing the dynamics of risk determinants.

In the third phase, the probability of occurrence, 1/T (where T is the return time), of fluvial and pluvial flooding is computed for each flood scenario. The area exposed to fluvial flooding, according to the hazard scenarios, can be identified using a hydraulic numerical model. In this study, the HEC–RAS software was used for this purpose, in a one-dimensional (1-D) configuration [11]. The model calculates the water surface elevations and flooded areas for different discharges, depending on the riverbed geometry. In unsteady simulations conducted using measured hydrographs, the geometry

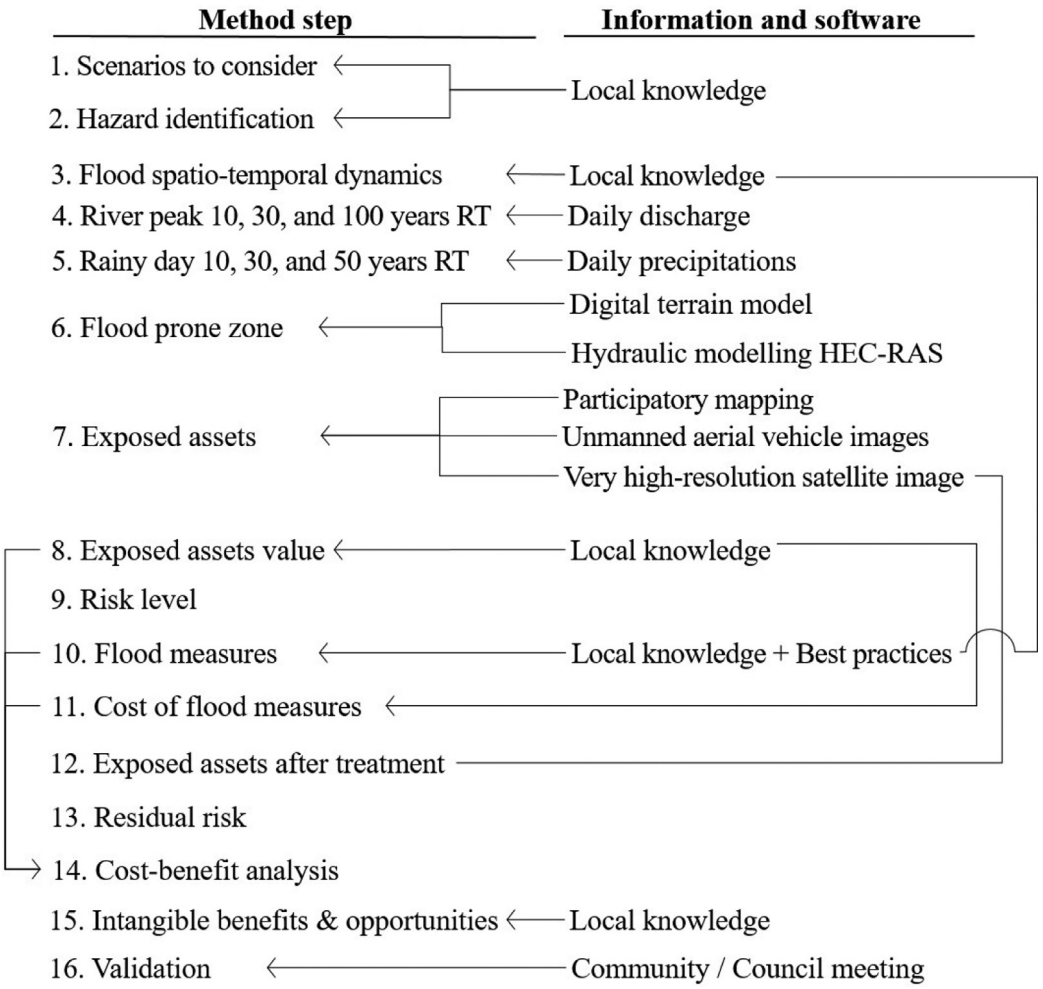

Fig. 1. Flowchart of flood risk assessment.

derived from a digital terrain model (DTM) allows the estimation of the propagation and submergence times during fluvial flooding.

Areas exposed to pluvial flooding can be identified using HEC–RAS in a two-dimensional (2-D) configuration. However, in some contexts, a pluvial flood is of very short duration and limited depth. In these cases, it is preferable to estimate the potential damage in relation to the damage produced by recent events with known intensities.

Exposed assets within fluvial flood-prone zones are identified. In rural areas, these are mainly houses, latrines, barns, schools, warehouses, infrastructure (e.g., wells, boreholes, fountains, and photovoltaic plants), and crops. Crops should be identified in the season in which flooding is likely to occur because, in other seasons, they may not be present or may be replaced by crops of different values. Depending on the number of assets and the accessibility of the flood zone, various methods can be used for asset identification, including direct check on site, photo interpretation of open-access satellite imagery at VHR, and imagery from UAVs. For extensive areas, the use of UAVs is the quickest and least expensive method, because it does not require an onsite check if the visual photo interpretation is performed by an operator who knows the context (or has visited the site).

UAV-derived information can also be retrieved using artificial intelligence techniques, permitting even faster analysis. UAV imagery can be obtained even during the wet season, whereas VHR satellite imagery may not be available because of cloud cover. Finally, UAV images make it possible to clearly distinguish buildings with metal roofs from those with earthen roofs. Many countries in the Global South now use specialised local UAV operators.

Once flood-prone assets have been identified, their replacement or repair values must be estimated. For this purpose, the stage-damage function and flow velocity are used for all assets that can partially resist the flood. The estimation of crop damage, in turn, considers the flooding duration and water depth. To estimate the potential damage, a standard housing unit can be used, the replacement cost of which should be determined based on on-site discussions with the community. In some countries, cost estimation of standard rural buildings is available. The risk level is obtained by multiplying the hazard by the potential damage under each flood scenario. In rapidly changing rural contexts, it is necessary to broaden the scenarios. A flood probability with a return period of 100 years will be affected by changes in land use, land cover, and climate, and this will increase the probability of occurrence of, otherwise, rare events in the future.

In the fourth phase, actions that would reduce the flood risk are identified and ordered according to the following criteria: local knowledge of the action, relevance to flood risk, acceptance by the community, availability of local skills, willingness to collaborate, community resources, environmental impact, maintenance requirements, and positive fallouts. The community evaluates each action, providing a score to each criterion. Actions are then prioritised according to the total score received.

The cost-benefit analysis (CBA) is developed by considering the difference between the potential damage before (D) and after treatment (Dt), compared to the cost of treatment (C), i.e., $B/C = (D - Dt)/(1-r)^n \; / \; C/(1-r)^n$ where r is the discount rate and n is the number of years. Values exceeding 1 express the benefit of risk treatment in monetary terms [12].

However, intangible benefits are also considered as opportunities, e.g., recession agriculture, which the lack of water would not allow to develop.

Validation

Context

The improved method for fluvial and pluvial FRA was applied to the period between 2018 and 2020 to the four main settlements along the Sirba River, which is one of the major right-bank tributaries of the Middle Niger River [13,14] (Fig. 2).

These settlements are, from upstream to downstream, Touré (4,065 inhabitants in 2012, 0.6 km^2 built-up area in 2018), Labra Birno (4,713 inhabitants, 0.7 km^2), Garbey Kourou (4,643 inhabitants, 0.6 km^2) and Tallé (2,603 inhabitants, 0.5 km^2). Data and images for Touré are presented below. Data for the other settlements are freely accessible from the Mendeley repository.

Frequent, moderate, and rare scenarios of fluvial and pluvial flooding were considered. Two variants were considered for each scenario: a baseline without risk reduction (B) and one with risk treatment (T). This resulted in a total of 12 scenarios.

Risk identification

Risk identification was carried out by combining local knowledge with the results of analysing the river discharge and precipitations series by using VHR satellite images accessible from Google Earth Pro and captured by UAVs.

Meetings with communities provided insights that purely probabilistic methods could not have provided on the hazard that each community was exposed to, as well as flood dynamics, causes of flood damage, and the critical threshold at which damage is initiated. For example, communities note that pluvial floods are not necessarily caused by extreme rainfall. Two successive days of average rainfall can create the conditions for catastrophic flooding: the first rainfall saturates the soil, and the second, which can no longer infiltrate the ground, generates so much runoff that it floods the settlement (Table 1).

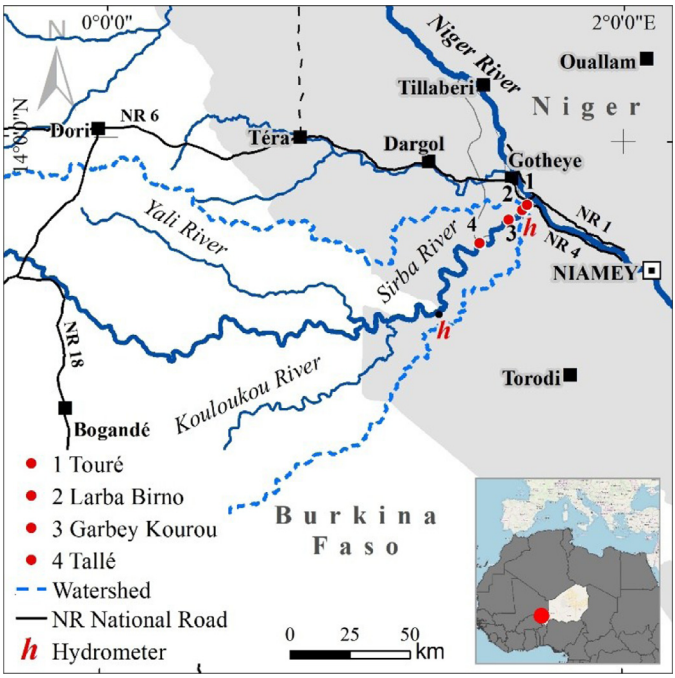

Fig. 2. Transboundary watershed of the Sirba River and the four rural settlements.

Table 1
Causes of flood damage in Touré.

Causes of flood damage	Touré
Heavy rain	•
Two consecutive rainy days	•
Runoff	•
Reduction of vegetation in the catchment	•
Lack of drainage	•
Rainwater stagnation	•
Settlement expansion in flood-prone area	•
Housing vulnerability (adobe construction)	•
Assets cannot be displaced (boreholes, wells)	•

Meetings were accompanied by participatory mapping (Fig. 3) and asset inspections that allowed the recognition of how assets visible from satellite or UAV images correspond to features on the ground.

The discharge values of the Sirba River were recorded at the Garbey Kourou gauge for the period of 1956–2020, and those of the Niger River were recorded at the Niamey gauge for the period of 1956–2020. The annual peak discharge of the Sirba River shows a significant increase after 2010 (Fig. 4).

The Touré built-up area increased at an average annual rate of 5.9% between 2008 and 2018. Three hazard scenarios were analysed, with frequent, moderate, and rare probabilities of occurrence, according to the expected damage magnitude defined in 2002 by a multidisciplinary team composed of personnel from the Ministry of Hydraulics, Ministry of Agriculture, the National Directorate for Meteorology, civil protection services, AGRHYMET, and the Niger River Basin Authority. These three

Fig 3. Participation in mapping of flood assets in Touré.

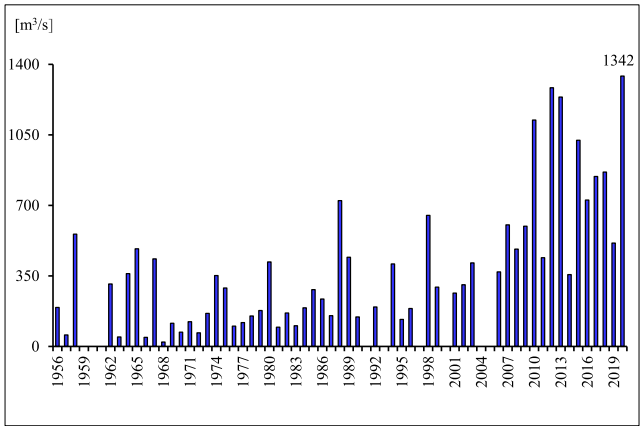

Fig. 4. Annual maximum discharge at Garbey Kourou gauging station [15].

Table 2
Flood hazard for the Sirba riverine communities.

Flood hazard	Probability (%)	Return time (Years)	Discharge (m^3/s)	Rainfall (mm)
Sirba overflow	10	10	761	
	3	30	1365	
	1	100	2120	
Niger backwater	5	20	2238	
	10	10		90
Pluvial	3	30	-	100
	2	50		200

scenarios correspond to hazard thresholds with return periods of 10, 30, and 100 years and discharges (Q max) of 761, 1365, and 2238 m^3/s, respectively (Table 2).

Some assets were not evident in the UAV images, and even less so in the VHR satellite images if one does not know what to look for. This is the case with boreholes, wells, and fountains, which discussions with communities reveal to be often flooded and regularly out of service during the rainy season (Fig. 5).

Fig. 5. Fountain flooded during rainy season in Larba Birno.

Table 3
Integration of local and scientific knowledge into FRA.

FRA Step	Knowledge	
	Local	Technical-Scientific
Hazard	Pluvial relevance, critical rain	River discharge, precipitations
Exposure	Flood prone boreholes, fountains, photovoltaic plants, wells	Assets location
Damage	Drivers, assets value	Tangible damages
Risk level		Scenarios
Risk reduction	Feasibility of measures	Effective risk reduction
Risk evaluation	Intangible benefits, opportunities	CBA, opportunity analysis

Knowledge integration is therefore systematic and occurs at each step of the FRA (Table 3).

Risk analysis

Based on the recorded discharge values, the probability of flooding due to the effects of overflow of the backwaters of the Sirba and Niger Rivers were calculated using a generalized extreme value probability distribution.

Flood-prone areas have been identified using hydraulic numerical model simulations conducted using the Hydrologic Engineering Centre–River Analysis System (HEC–RAS), version 5.0.6 [11]. The yellow, orange, and red colours used on the hazard maps represent flood-prone areas with frequent, moderate, and rare probabilities of occurrence, respectively.

The river geometry was derived from a digital terrain model (DTM) with a horizontal resolution of 10 m, detailed by a GPS-based-rover on-site topographic survey. The survey was conducted using real-time kinematic and precise point positioning techniques and resulted in 147 river cross sections with a vertical accuracy of approximately 10 cm. The surface roughness of the riverbed cross sections depends on the size and shape of the sediments. Therefore, the riverbed granulometry was evaluated using an object detection algorithm [16], which analyses the photographs taken during the land surveys to determine the mean size of the coarse material. Manning's coefficients assumed for the roughness of the river zones ranged from 0.033 n ($s/m^{1/3}$) for irregular and rough sections to 0.1 n

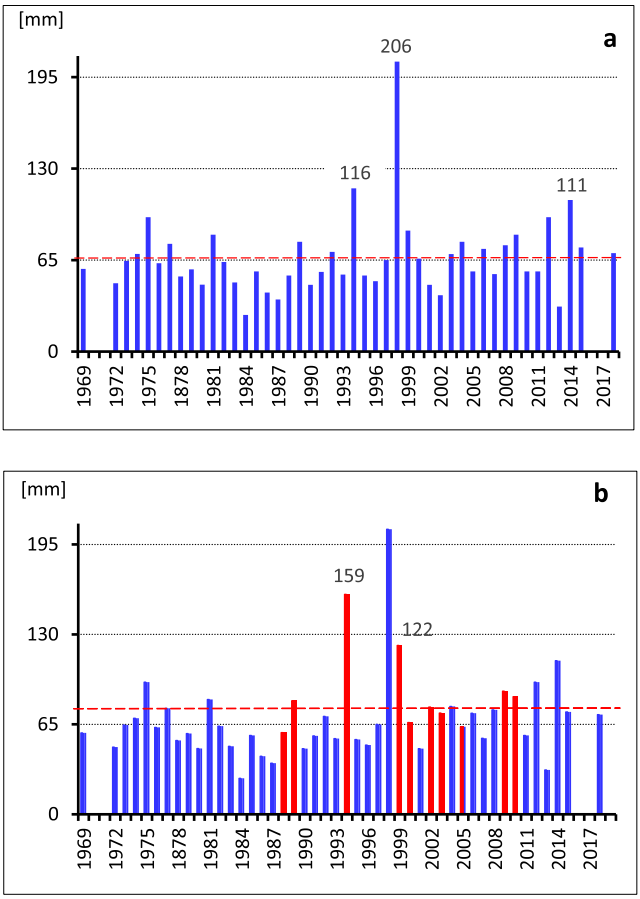

Fig. 6. Fifty years of maximum daily rainfall (a) and for two consecutive days (b) at Gothèye rain gauge. The differences between the two distributions are highlighted in red (b).

($s/m^{1/3}$) for heavy stands of timber [17]. The downstream flood boundary conditions were imposed from the hydraulic water levels of the Niger River. The hydraulic numerical model was calibrated with the hydraulic levels measured at the Bossey Bangou and Garbey Kourou hydrometric stations and in the four rural settlements during the rainy season in 2018 [13]. The boundaries of flooded areas were validated during the 2020 flood, which reached the highest discharge level in the available historical series. The propagation times from the Bossey Bangou hydrometer (108 km upstream from the Sirba–Niger confluence) to Touré, Larba Birno, and Garbey Kourou–Tallé were 20, 26, and 28 h respectively. These are sufficiently long times to activate the emergency warning system (EWS) to alert the villages downstream, even if the flood occurs during the night [18].

The backwater of the Niger River is a devastating phenomenon that only affects the community of Tallé. Its return time is calculated from the dataset of river flows recorded at the river gauge in Niamey. The daily rainfall is obtained from recordings at the Gothèye rain gauge, located 30 km from Touré. Frequent, moderate, and rare rainfall probabilities are considered to have return times of 10, 30, and 50 years, respectively, and intensities of 90, 100, and 200 mm, respectively. Instead of using maximum daily rainfall (Fig. 6a), the accumulation of two consecutive days of rainfall (Fig. 6b) reported by communities as an event likely to generate catastrophic flooding was used.

Table 4
Number of houses exposed to flood in Touré in 2018.

Hazard	Level	Houses in flood-prone zone (n.)	Houses exposed to heavy rainfall (n.)
Sirba River overflow	Yellow	0	
	Orange	3	
	Red	79	
Niger River backwater	Red	-	
Pluvial	Yellow		1903
	Orange		1903
	Red		1903

The identification of fluvial flood-prone assets was conducted using two methods, depending on the exposure amount and asset accessibility. The first method was used for Tallé and Garbey Kourou and involved the reconnaissance of all identifiable buildings on VHR satellite images, which were freely accessible from Google Earth Pro. After the coordinates of each asset were provided to a local operator, the masonry materials and asset usage were identified through a ground survey. For fields, the type of crop (e.g., orchard, rain-fed crops, vegetables) and the coordinates of the fenced vegetable gardens were recorded. The second method was used for the two largest and most remote settlements, i.e., Larba Birno and Touré, and involved photographing the two settlements using an UAV. Two optical sensors were mounted on the UAV: a Sony ILCE-5100 camera (24.3 Mpx) and an experimental sensor (5 Mpx) created with a Raspberry Pi computer and two Raspberry Pi 2 cameras [19]. The Sony-ILCE-5100 is a regular camera that captures information from the visible part of the electromagnetic spectrum (red–green–blue), whereas the experimental sensor captures the near-infrared part of the electromagnetic spectrum (NIR). The sensors were not carried by the UAV simultaneously because of their large weights and because their different characteristics required different specific flight settings (i.e., the height and speed of flight) to obtain imagery with a similar ground resolution. Therefore, two flights were conducted at each settlement on the 14th and 15th of September 2018, at 270 and 120 m above ground level for the RGB and NIR cameras, respectively. The data collected were processed with a Structure from Motion Workflow. From the resulting 3D model, one RGBN orthophoto of 6 cm/px and one RGB orthophoto of 4 cm/px were obtained for each settlement. The exposed assets were identified via visual photo interpretation of the orthophotos at a 4-cm resolution. Those images allowed the identification of houses with earthen roofs and houses with iron sheet roofs, as well as latrines, barns, boreholes, wells, fountains, photovoltaic plants, long-lasting ponds, rain-fed crops, and irrigated crops, which cannot be clearly identified in VHR satellite images available from Google Earth Pro (Figs. 7–8 and Table 4).

UAV overflights should be carried out in early to mid-September, when rain-fed crops are still in place. The building damage estimate does not depend on the stage-damage function nor on the flow velocity. This is because the majority of the houses are built from adobe masonry, and thus collapse once they are flooded. The flood duration and the depth of the water were considered to estimate the damage to the crops.

Compared to rural settlements in the Dosso Region (Niger) [20], in the case of Touré, pluvial inundation results in shallow flash floods of short durations and speeds. In this case, the damage is mainly caused by the impact of the rain on the roofs and by the formation of puddles that last for several weeks and can wash over the buildings and cause them to collapse (Fig. 9).

Visual photointerpretation of UAV imagery showed that 96% of the dwellings had earthen roofs. Based on the 30 houses that collapsed after a rainfall of 148 mm in 2017, it was estimated that 41, 20, and 18 houses could collapse following rainfalls of 200, 100, and 90 mm, respectively. In addition, the orthophotos produced by the images captured using UAV showed 12 puddles surrounded by 25 houses, 15 latrines, and 4 barns that could be lapped, according to the red scenario.

The replacement values of the houses were estimated through community meetings, based on the construction cost of a standard 24-m^2 adobe house, latrine, shower, and barn (Tables 5 and 6). The high water lasts for a long time; thus, submerged crops do not survive a flood. The crop values were calculated based on the prices in the local market and yields estimated by the Departmental

Fig. 7. (top) VHR satellite image freely available from Google Earth Pro and (bottom) a VHR image taken from UAV of flood-prone assets in Touré.

Table 5
Value of exposed assets.

Asset	Unit	Thousand €
Adobe house	1	576
Latrine	1	70
Barn	1	143
Well disinfection	1	122
Commercial vegetable crops	0.01 km^2	200
Millet	0.01 km^2	374
Paddy	0.01 km^2	557

Directorate for Agriculture of Gothèye and integrated with statistics from the Ministry of Agriculture and Livestock [21].

The risk level is calculated for each hazard (backwater, fluvial, pluvial floods) according to scenario B (Table 6).

Risk evaluation

The evaluation uses residual risk, CBA, intangible benefit, and opportunity analysis. Community meetings to identify and prioritize actions were held on the 25th and 26th of June 2019 and were attended by the village chief, a representative of the women farmers, a community observer of

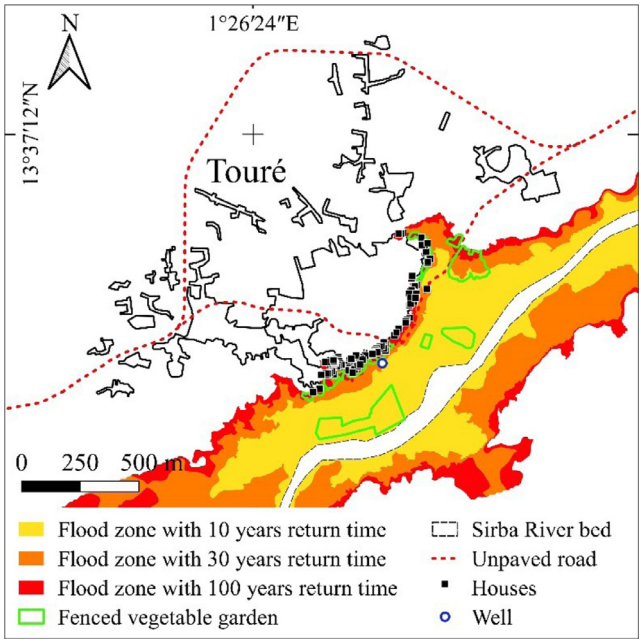

Fig. 8. Hazard map and exposed assets in Touré.

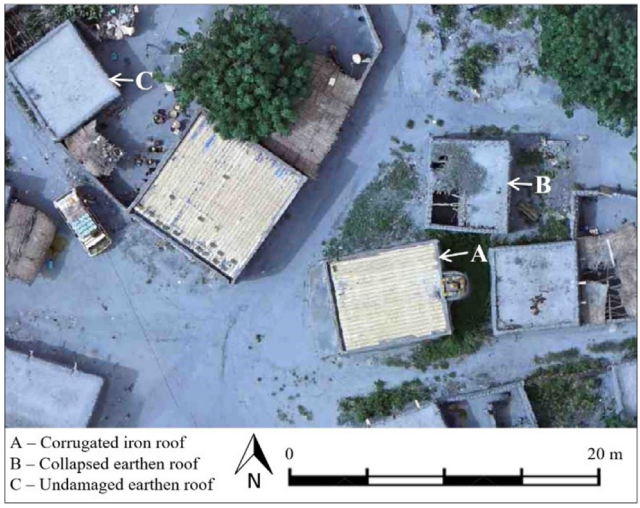

Fig. 9. Recognition of the vulnerability of the Touré roofs from orthophotos taken in September 2018 by UAV.

the EWS, agriculture and environment officials of the municipality of Gothèye, the mayor, and representatives of the municipal council, the National Directorate for Meteorology, and the National Council for the Environment and Sustainable Development. The integration of local and scientific knowledge into the risk analysis and the CBA facilitated the identification and localisation of specific risk treatment that would not have been possible with participatory or technical analysis alone.

Table 6
Risk level in Touré according to scenario.

Scenario		Hazard (%)	Damage (€)	Risk (€)	
Fluvial	Yellow B	10	8033	803	
	Yellow T	10	427	42	5
	Orange B	3	10045	301	
	Orange T	3	625	19	6
	Red B	1	62530	625	
	Red T	1	991	10	2
Pluvial	Yellow B	10	26639	2664	
	Yellow T	10	0	0	0
	Orange B	6	27782	1667	
	Orange T	6	0	0	0
	Red B	2	39215	784	
	Red T	2	0	0	0

Table 7
Costs of risk reduction in Touré according scenario.

Action	Actions according scenario			Cost unit (€)	Cost (€) according scenario		
	10 yrs	30 yrs	100 or 50 yrs		10 yrs	30 yrs	100 or 50 yrs
Garden fence	0.01 km^2	0.01 km^2	0.01 km^2	4948	4948	4948	4948
Household to resettle	0	3	82	915	0	2735	75030
Red zone marking	4	4	4	183	732	732	732
Contingency plan	1	1	1	2500	2500	2500	2500
Fluvial risk reduction					8180	10915	83210
Latrine rise	18	20	25	70	1260	1400	4623
House retrofitting	18	20	41	169	3042	3380	6929
Pond remediation	327 m^2	327 m^2	327 m^2	1371	1371	1371	1371
Contingency plan	1	1	1	2500	2500	2500	2500
Pluvial risk reduction					8173	8651	15423

Table 8
CBA results for Touré.

Flood	RT (years)	Benefit (€)	Cost of treatment (€)	B/C
Fluvial	10	7606	8180	0.93
	30	9420	10915	0.86
	100	61539	83210	0.74
Pluvial	10	26639	8173	3.26
	30	27782	8651	3.21
	50	39215	15423	2.54

The information gathered from the analysis allowed the identification of settlement-specific risk reduction actions, such as marking the flood zone limits, adopting contingency plans, organising flood drills, promoting the construction of latrines above the flood level, raising the floors of wells and photovoltaic plants, resettling households from orange and red zones to lower-risk zones, retrofitting adobe housing, pond remediation, and maintenance of early warning system. Estimating the cost of these actions again requires the participation of the community and municipal officials (Table 7).

Furthermore, as flooding provides opportunities for recession agriculture, horticultural crops should be fenced to protect them from stray animals (Fig. 10).

These actions make it possible to estimate how much the risk is lowered as a result of their implementation. The benefit-to-cost ratio was calculated to appreciate in monetary terms the convenience of multi-hazard risk treatment. These actions are feasible within a single year. It is therefore not necessary to include the discount rate in the CBA formula (Table 8).

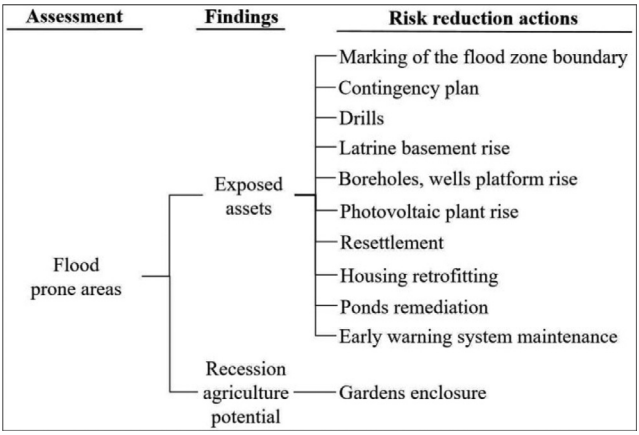

Fig. 10. Risk analysis–evaluation nexus.

Table 9
Intangible benefits of risk reduction and flood opportunities in Touré.

Intangible benefits	Opportunities
Risk awareness	Recession farming
Reduction in water supply duties	Commercial gardening
Fluvial flood early warning	Income opportunities for women
Public health improvement	

To make decisions to deal with or accept the risk, the CBA results were integrated with an assessment of the intangible benefits and opportunities that can sometimes yield important benefits for the community (Table 9).

Limits

The first limitation of the method used in this study is the use of a UAV for the VHR imagery collection. Indeed, although UAV data can provide a new level of detail for use in the detection of flood-prone assets, special flight permission must be obtained from the National Civil Aviation Agency of Niger, which can require a long time (even months) to obtain and might not be granted in cases of areas considered sensitive by the national government. Furthermore, UAV flights require payment of very expensive overflight fees. Such uncertainties and costs affect the affordability and convenience of UAV flights in these areas. Satellite data can be a convenient alternative to UAV flights. VHR satellite providers (such as Maxar, http://www.maxar.com/) offer many data options with spatial resolutions of a few centimetres. For example, the World View constellation provides panchromatic imagery with 0.30-m spatial resolution every 1–4 days, and historical data for the study area are available from 2014 on (World View-3). VHR satellite datasets have largely been applied in planning and natural hazard monitoring [22–23]. New algorithms to enhance the spatial resolution to 0.15 m in panchromatic imagery have recently been developed and ensure even better detection of ground features [24]. In contrast to UAV, satellite image availability is highly dependent on lack of cloud cover, but it is possible to combine temporally close images to minimise this limitation. VHR imagery at resolutions of less than 0.30 m pixels are available at moderate cost, and their use in FRAs in the Global South has been little explored.

The second limitation of the method used in this study is that it does not consider service interruptions of boreholes, wells, fountains, photovoltaic plants, and markets during floods.

Conclusion

In the Global South, FRAs usually consider only one hazard at time. Flood-prone areas, enclosed assets, and risk-reducing actions appropriate to the characteristics of individual settlements are also too often missing. Therefore, FRAs are not particularly useful in informing decision-making on flood risk reduction. More accurate FRAs should systematically include local knowledge and exploit the options offered by new technologies.

The use of images captured by UAVs reduces the time and cost of asset identification but should be preceded by a thorough discussion with the community and a field visit to preliminarily identify the assets to be searched in the images.

Treating risk lowers its level from 100 points in the absence of risk treatment to 2–6 points after treatment. Fluvial risk is reduced by moving assets out of exposed areas, and pluvial risk is reduced by protecting assets. It pays to treat the risk in all pluvial scenarios (b/c = 1.32 to 3.26) except the fluvial scenarios (b/c = 0.70 to 0.93). The method used in this study is innovative in its systematic integration of local and scientific knowledge, in the techniques used to identify assets, in the risk level scenarios considered, and in the intangibles benefits and opportunities for rural development offered by flooding, which is generally considered to be a purely adverse event. This method can be replicated in any context where decision making is needed to support flood risk reduction planning [25].

Declaration of Competing Interests

The authors declare that they have no known competing financial interests or personal relationships that could have appeared to influence the work reported in this paper.

Acknowledgments

The authors thank the AICS ANADIA 2.0 project for supporting the assessment methodology and its validation in the four rural settlements along the Sirba River. They also thank the National Directorate for Meteorology in Niger, the Ministry of Water and Sanitation, the prefect and mayor of Gothèye, and local communities for supporting the implementation of the field activities.

References

[1] C-J. Li, Y-Q Chai, L-S. Yang, H-R. Li, Spatio-temporal distribution of flood disasters and analysis of influencing factors in Africa, Nat. Haz. 82 (2016) 721–731, doi:10.1007/s11069-016-2181-8.
[2] United Nations, in: Sendai Framework for Disaster Risk Reduction, 2015-2030, UNDRR, Geneve, 2015, p. 32. -2030.
[3] A. Díetz-Herrero, J. Garrote, Flood risk analysis and assessment, applications and uncertainties: A bibliometric review, Water 12 (2020) 2050, doi:10.3390/w12072050.
[5] Y. Yang, M.L. Roderick, D. Yang, Z. Wang, F. Ruan, T.R. McVicar, S. Zhang, H.E. Beck, Streamflow stationary in a changing world, Environ. Res. Letters 16 (2021) 064096 (in press), doi:10.1088/1748-9326/ac08c1.
[6] P. Nakawuka, S. Langan, P. Schmitter, J. Barron, A review of trends, constraints and opportunities of smallholder irrigation in East Africa, Glob. Food Security 17 (2018) 196–212, doi:10.1016/j.gfs.2017.10.003.
[7] E. Mavhura, S.B. Manyena, A.E. Collins, D. Manatsa, Indigenous knowledge, coping strategies and resilience to floods in Muzarabani, Zimbabwe, Int. J. Disaster Risk Reduc. 5 (2013) 38–48, doi:10.1016/j.ijdrr.2013.07.001.
[8] International Organization for StandardizationISO 31010 Risk Management-Risk Assessment Techniques, IEC-ISO, Geneve, Switzerland, 2009.
[9] W.N. Adger, L. Brown, S. Surminski, Advances in risk assessment for climate change adaptation policy, Phil. Trans. R. Soc A (2018) 376, doi:10.1098/rsta.2018.0106.
[10] M.S. Kappes, M. Keiler, K. von Elverfeldt, T. Glade, Challenges of analyzing multi-hazard risk: A review, Nat. Hazards 64 (2012) 1925–1958, doi:10.1007/s11069-012-0294-2.
[11] G.W. Brunner, HEC-RAS River Analysis System: Hydraulic Reference Manual Version 5.0; US Army Corps of Engineers-Hydrologic Engineering Center (HEC), Davis, CA, USA, 2016.
[12] R. Mechler, Reviewing estimates of the economic efficiency of disaster risk management: opportunities and limitations of using risk-based cost-benefit analysis, Nat. Hazards 81 (2016) 2121–2147, doi:10.1007/s11069-016-2170y.
[13] G. Massazza, P. Tamagnone, C. Wilcox, E. Belcore, A. Pezzoli, T. Vischel, G. Panthou, M.H. Ibrahim, M. Tiepolo, V. Tarchiani, M. Rosso, Flood hazard scenarios of the Sirba river (Niger): evaluation of the hazard thresholds and flooding areas, Water 11 (5) (2019) 1018, doi:10.3390/w11051018.
[14] M. Tiepolo, M. Rosso, G. Massazza, D. Issa, E. Belcore, S. Braccio, Flood assessment for risk-informed planning along the Sirba river, Niger. Sust. 11 (15) (2019), doi:10.3390/su11154003.

[15] P. Tamagnone, G. Massazza, A. Pezzoli, M. Rosso, Hydrology of the Sirba river: updating and analysis of discharge time series, Water 11 (2019) 156, doi:10.3390/w11010156.
[16] M. Detert, V. Weitbrecht, Automatic object detection to analyze the geometry of gravel grains–a free stand-alone tool, in: River Flow, Taylor & Francis Group, London, UK, 2012, pp. 595–600. ISBN 978-0-415-62129-8.
[17] L.W. Mays, Water Resources Engineering, Wiley, Hoboken, NJ, USA, 2010 ISBN 978-0-470-46064-1.
[18] V. Tarchiani, G. Massazza, M. Rosso, M. Tiepolo, A. Pezzoli, M. Housseini Ibrahim, G.L. Katiellou, P. Tamagnone, T. De Filippis, L. Rocchi, V. Marchi, E. Rapisardi, Community and impact based early warning system for flood risk preparedness: The experience of the Sirba River in Niger, Sust 12 (2020) 1802, doi:10.3390/su12051802.
[19] E. Belcore, M. Piras, A. Pezzoli, G. Massazza, M. Rosso, Raspberry PI 3 multispectral low-cost sensor for UAV based remote sensing. Case study in South-West Niger, Int. Arch. Photogramm. Remote Sens. Spat. Inf. Sci. 4213 (2019) 207–214, doi:10.5194/isprs-archives-XLII-2/W13-207-2019.
[20] M. Tiepolo, A.S. Adamou, E. Fiorillo, A. Galligari, G.L. Katiellou, H. Ibrahim Mohamed, G. Massazza, A.M. Tankari, PRRI–Plan de réduction du risqué d'inondation de Gagila et de Takouidawa villages administratifs de la commune rurale de Kiéché, Région de Dosso, ANADIA 2.0 Project, Report 16, 2021, doi: 10.13140/RG.2.2.31221.09440.
[21] Republic of Niger, Ministry of Agriculture and Livestock. Rapport d'évaluation préliminaire des récoltes et résultats provisoires de la campagne agricole d'hivernage 2018, Ministère de l'Agriculture et de l'Élevage, Niamey, Niger, 2019.
[22] S.I. Jiménez-Jiménez, W. Ojeda-Bustamante, R.Ernesto Ontiveros-Capurata, M. Marcial-Pablo, Rapid urban flood damage assessment using high resolution remote sensing data and an object-based approach, Geomatics, Nat. Hazards Risk 11 (1) (2020) 906–927, doi:10.1080/19475705.2020.1760360.
[23] M. Al-Amin Hoque, S. Phinn, C. Roelfsema, I. Childs, Tropical cyclone disaster management using remote sensing and spatial analysis: a review, Int. J. Disaster Risk Reduc. 22 (2017) 345–354, doi:10.1016/j.ijdrr.2017.02.008.
[24] Maxar, Earth Intelligence. Maxar Technologies, Westminster, CO, USA, 2020, https://blog.maxar.com/earth-intelligence/2020/introducing-15-cm-hd-the-highest-clarity-from-commercial-satellite-imagery.
[25] M. Tiepolo, E. Belcore, S. Braccio, H. Ibrahim Mohamed, S. Issa, G.L. Katiellou, G. Massazza, M. Rosso, Plan de réduction du risque d'inondation de Touré, village administratif de la Commune de Gothèye, Région de Tillabéri, Projet ANADIA 2.0, Rapport 23, 2021, doi: 10.13140/RG.2.2.36611.43048.
[26] M. Tiepolo, A. Galligari, Urban expansion-flood damage nexus: Evidence from the Dosso region, Niger, Land Use Policy 108 (2021) 105547, doi:10.1016/j.landusepol.2021.105547.